ELSEVIER

Journal of Molecular Catalysis A: Chemical 175 (2001) 227–239

JOURNAL OF MOLECULAR CATALYSIS A: CHEMICAL

www.elsevier.com/locate/molcata

Probing polyfunctional nature of vanadyl pyrophosphate catalysts: oxidation of 16 C_4 molecules

V.V. Guliants*, S.A. Holmes

Department of Chemical Engineering, University of Cincinnati, Cincinnati, OH 45221-0171, USA

Received 9 January 2001; received in revised form 18 April 2001; accepted 8 May 2001

Abstract

A vanadyl pyrophosphate catalyst, $(VO)_2P_2O_7$, was investigated for its ability to selectively oxidize 16 C_4 probe molecules, including hydrocarbons, alcohols, diols, and five-membered heterocycles, to maleic anhydride in a fixed bed microreactor. It was observed that besides linear-chain hydrocarbons and five-membered heterocycles previously studied, the butanols and butanediols can also be selectively oxidized into maleic anhydride. This demonstrates the existence of new selective oxidation pathways of organic molecules over the VPO catalysts. A novel *cis*-(su)peroxo-oxovanadium(V) dimeric active surface site is proposed for the (1 0 0) plane of $(VO)_2P_2O_7$. New selective oxidation pathways of organic molecules over the $(VO)_2P_2O_7$ catalyst involving the proposed active surface site are described. The proposed pathways are consistent with both the redox behavior of V^{IV} and V^V and the known organic chemistry of the C_4 probe molecules.

Keywords: Vanadyl pyrophosphate; Selective oxidation; Mechanism; Active site; Oxidation state

1. Introduction

Vanadyl pyrophosphate has been identified as the main crystalline phase present in the most selective and active VPO catalysts for *n*-butane oxidation to maleic anhydride [1]. However, various crystalline and disordered V^{IV}/V^V phosphate phases are also observed depending on the redox properties of reactants, the time on stream, and the reaction temperature as the results of facile interconversion the V^V and V^{IV} oxidation states [1–6]. The limited known physical characterization coupled with the complex solid-state chemistry of vanadium phosphates has led to much controversy in the literature concerning the nature of the active phase in *n*-butane oxidation and the identity of the active surface sites involved in different steps of the catalytic reaction [1–6]. For example, the active surface sites for the selective oxidation of *n*-butane were associated in the past with (i) coherent interfaces between slabs of the (1 0 0) planes of various $VOPO_4$ phases and $(VO)_2P_2O_7$ [7], (ii) a mixture of well-crystallized $(VO)_2P_2O_7$ and amorphous $VOPO_4$ phases involving corner-sharing VO_6 octahedra [8], (iii) the domains of γ-$VOPO_4$ supported on a $(VO)_2P_2O_7$ matrix [9], (iv) the $VO(PO_3)_2$ phase [10,11], (v) the $VOPO_4$ "X1" phase [12], (vi) the surface line defect V^{III} species present in the (1 0 0) surface of $(VO)_2P_2O_7$ [13,14], and (vii) limited and controlled amount of V^V species present in the (1 0 0) surface of $(VO)_2P_2O_7$ [4,5,15–20].

The most selective and active equilibrated VPO catalysts preferentially expose the (1 0 0) planes of $(VO)_2P_2O_7$ [1–5]. The models of *n*-butane oxidation on the VPO catalysts proposed to date are based on

* Corresponding author. Tel.: +1-513-556-0203; fax: +1-513-556-3473.
E-mail address: vadim.guliants@uc.edu (V.V. Guliants).

1381-1169/01/$ – see front matter
PII: S1381-1169(01)00222-9

the hypothetical active *trans*-oxo vanadium(IV) dimer sites present in the (1 0 0) surface plane. The following types of hypothetical active sites have been proposed to exist on this surface plane [21]: (i) Brønsted acid sites, probably –POH groups, (ii) Lewis acid sites, probably V^{IV} and V^{V}, (iii) one electron redox couple, V^{V}/V^{IV}, V^{IV}/V^{III}, (iv) two electron redox couple, V^{V}/V^{III}, (v) bridging oxygen, V–O–V, V–O–P, or VO(P)V, (vi) terminal oxygen, V^{V}=O, V^{IV}=O, and (vii) activated molecular oxygen, η^1-peroxo and η^2-superoxo species. In an isotopic exchange study, Pepera et al. [22] found that fast oxygen exchange on VPO catalysts can only occur in the near surface region. Every two surface vanadium atoms are capable of activating one molecule of dioxygen, while the bulk of the catalyst does not participate in *n*-butane oxidation. Wang et al. [20] have recently confirmed these observations and further demonstrated that selective oxidation of *n*-butane over VPO catalysts takes place via a Mars–van Krevelen mechanism in which the VPO catalyst surface cations cycle under steady state reaction conditions between V^{IV} and V^{V}.

The contemporaneous removal of two methylene hydrogen atoms from the carbon atoms in the second and third positions in *n*-butane is the first and rate-limiting step in selective oxidation to maleic anhydride [1,20–22]. Guliants [23] employed the model supported vanadia catalysts and obtained evidence that this reaction is more efficient over multiple vanadium sites, which provides some support to the models of the active surface sites based on the vanadyl(IV) dimers [1–5,21]. Butenes, butadiene, and furan, which were observed under high vacuum conditions in a temporal analysis of products (TAP) reactor [18,19,24] were suggested as the hypothetical reaction intermediates. However, these transient species are not observed under typical reaction conditions. Because very limited insights have been gained from the studies of the reaction intermediates during *n*-butane oxidation, the proposed models of *n*-butane oxidation to maleic anhydride suffer from a lack of mechanistic detail.

In the present study, we study the oxidation of 16 C_4 probe molecules, including *n*-butane, over the equilibrated $(VO)_2P_2O_7$ catalyst and provide additional insights into the polyfunctional nature of the VPO catalysts. Furthermore, we propose a new V(IV) dimeric site present in the surface (1 0 0) planes of $(VO)_2P_2O_7$ and detailed reaction pathways for the oxidation of the C_4 molecules over these surface active sites, which are consistent with the redox chemistry of the $V^{IV,V}$ oxidation states and the known organic chemistry of the C_4 probe molecules.

2. Experimental

2.1. Synthesis

The organic precursor of the VPO catalysts was prepared by reacting vanadium pentoxide (Aldrich) with 100% *ortho*-phosphoric acid (Aldrich) (synthesis $P/V = 1.16$) in 10:1 mixture of *i*-butanol and benzyl alcohol at reflux for 16 h according to the reported procedure [25]. The blue solid was isolated by filtration, washed with *i*-butanol and acetone, and dried in air at 383 K overnight. The XRD and Raman confirmed the composition of the precursor to be $VOHPO_4{\cdot}0.5H_2O$ [4]. The TGA weight loss in nitrogen at 873 K (10.9%) agreed well with the theoretical value for stoichiometric transformation of $VOHPO_4{\cdot}0.5H_2O$ into $(VO)_2P_2O_7$ (10.6%).

2.2. Kinetic studies

Approximately 1 g of the 212–355 μm fraction of the precursor was placed in the catalytic microreactor, and activated in situ at 708 K in 1.2% *n*-butane in air. The kinetic measurements and the analysis of products by gas chromatography are described in detail elsewhere [4]. The feed flowrate was fixed at 40 ml/min and the effluent samples were analyzed periodically until *n*-butane conversion and selectivity to maleic anhydride stabilized. It typically took between 2 and 4 weeks for a catalyst to reach steady state under such conditions, after which the selectivity–conversion curves were collected in 1.2% *n*-butane in air at 708 and 673 K. The curves obtained agreed well with those previously reported [25]. The temperature was then lowered to 633 K and liquid samples of various probe molecules were injected into flowing air at the microreactor inlet by high precision Harvard syringe pump to give the vapor concentration in air in the 1–4 vol.% range. The gaseous species, i.e. *i*-butane, *i*-butene, 1-butene,

cis- and *trans*-2-butene, were introduced similar to *n*-butane. The partial oxidation of *n*-butane at 673 K on this catalyst was checked periodically to confirm the stability of the active surface. The characterization of the used catalyst after kinetic experiments by XRD and Raman showed that it contained only vanadyl pyrophosphate [4].

3. Results

The total of 16 different species was employed in the present study shown in Tables 1–3. All the linear C_4 molecules and the five-membered heterocycles were oxidized to maleic anhydride (MA), although the yields obtained varied dramatically. Apart from

Table 1
Transformation of C_4 hydrocarbons over $(VO)_2P_2O_7$ catalyst at 633 K

Substrate (conversion, %)	Concentration (mol%)	Products (selectivity, mol%)
n-Butane (30)	1.2	Maleic anhydride (73) Acetic acid (3) Acrylic acid (1)
i-Butane (21)	1.2	Acetic acid (12), maleic anhydride (11) Acrylic acid (3), methacrolein (3) Methacrylic acid (2), acetone (1)
1-Butene (95)	1.3	Maleic anhydride (23), 1,3-butadiene (10) *Trans*-2-butene (8), acetic acid (7) *Cis*-2-butene (6), furan (3) Acrylic acid (1), methylethylketone (1)
Cis-2-butene (95)	1.3	Maleic anhydride (21), *trans*-2-butene (21) 1,3-Butadiene (17), 1-butene (12) Acetic acid (5), furan (3) Acrylic acid (1), methylethylketone (1)
Trans-2-butene (95)	1.3	Maleic anhydride (36), 1,3-butadiene (8) *Cis*-2-butene (6), 1-butene (5) Acrylic acid (2)
i-Butene (89)	1.3	Methacrolein (30), acetic acid (4) Acetone (2), methacrylic acid (2) Acrylic acid (1)

Table 2
Transformation of five-membered heterocycles over $(VO)_2P_2O_7$ catalyst at 633 K

Substrate (conversion, %)	Concentration (mol%)	Products (selectivity, mol%)
Tetrahydrofuran (100)	3.4	Maleic anhydride (74), acetic acid (8) Acrylic acid (2), furan (1) Ethylene (1)
2,5-Dihydrofuran (100)	4.0	Maleic anhydride (62), furan (17) Acetic acid (3), acrylic acid (1)
2,3-Dihydrofuran (100)	3.1	Maleic anhydride (37), acetic acid (5) Acrylic acid (4), ethylene (3) Furan (2)
γ-Butyrolactone (95)	2.7	Maleic anhydride (38), acrylic acid (21) Acetic acid (7), ethylene (1) Propylene (1)

Table 3
Transformation of alcohols and diols over $(VO)_2P_2O_7$ catalyst at 633 K

Substrate (conversion, %)	Concentration (mol%)	Products (selectivity, mol%)
1-Butanol (100)	2.6	Maleic anhydride (48), acetic acid (14) Acrylic acid (6), 1,3-butadiene (5) *Trans*-2-butene (4), *cis*-2-butene (3) 1-Butene (2), acetone (1) Ethylene (1), propylene (1)
2-Butanol (100)	2.7	Maleic anhydride (25), *trans*-2-butene (16) *Cis*-2-butene (12), 1,3-butadiene (13) 1-Butene (9), acetic acid (7) Furan (4), acetone (1) Acrylic acid (1)
1,4-Butanediol (100)	3.2	Maleic anhydride (93) Furan (2)
1,3-Butanediol (100)	2.3	Maleic anhydride (50), propylene (9) Acetic acid (9), 1,3-butadiene (8) Acrylic acid (4), ethylene (1)
1,2-Butanediol (100)	3.3	Maleic anhydride (40), acetic acid (25) Acrylic acid (13), furan (1) Ethylene (1), propylene (1)
i-Butanol (100)	2.5	Acetic acid (18), *i*-butene (14) Maleic anhydride (10), 1,3-butadiene (4) *Trans*-2-butene (3), *cis*-2-butene (2) Methacrolein (2), propylene (1)

MA, only traces of other partial oxidation products (acetic and acrylic acids) resulted from oxidation of *n*-butane (Table 1) in agreement with previous observations [1–3,21]. In the oxidation of 1- and 2-butenes, the yield of MA was lower than in the case of *n*-butane, and other partial oxidation products, such as furan, products of C=C and C–C bond scission and acetic and acrylic acids were observed. The VPO catalyst also catalyzed the isomerization and dehydrogenation of butenes also in accordance with previous results [1–3,21].

High selectivity to MA was observed in the oxidation of the two heterocyclic compounds, tetrahydrofuran and 2,5-dihydrofuran shown in Table 2. Traces of furan and ethylene, in addition to low levels of acetic and acrylic acids, were also observed for tetrahydrofuran oxidation. The yield of MA in the case of 2,5-dihydrofuran was somewhat lower due to formation of furan with 17 mol% yield. Oxidation of 2,3-dihydrofuran was less selective (37 mol% yield of MA), giving larger quantities of the total oxidation products. γ-Butyrolactone was also oxidized to MA with comparably low selectivity, in this case acrylic acid was formed with 21 mol% yield.

Oxidation of the linear chain C_4 alcohols (1- and 2-butanol) led to the products and yields similar to those in oxidation of 1- and 2-butenes (Table 3). However, in the case of 1-butanol, a higher yield of maleic anhydride was observed.

Different oxidation products and yields to MA were obtained in the case of the four linear chain C_4 diols. The VPO catalyst displayed remarkably high yield of MA in oxidation of 1,4-diol (93 mol%), and only small amounts of furan and complete oxidation products were detected. Considerably lower yield of MA was observed in the case of 1,2- and 1,3-diols. 1,2-Butanediol gave high yields of acetic and acrylic acids, while the oxidation of 1,3-diol led to appreciable amounts of butadiene and propylene.

The oxidation of the three skeletal isomeric molecules, *i*-butane (2-methylpropane), *i*-butene (2-methylpropene), and *i*-butanol (2-methyl-1-propanol), produced very different results compared to the oxidation of linear chain species. The rate of *i*-butane

oxidation was similar to that of *n*-butane and considerably lower than in the case of all other, more reactive species shown in Table 1. No alkenes, i.e. ethylene, propylene, and *i*-butene, were detected. *i*-Butane gave mostly the products of complete oxidation, as well as the expected partial oxidation products: acetic, acrylic, and methacrylic acids, methacrolein and acetone. Surprisingly, the VPO catalyst showed some selectivity to MA even in this case (11 mol%). The oxidation of *i*-butene led to the expected partial oxidation products: acetic, acrylic, and methacrylic acids, methacrolein and acetone. In the case of *i*-butanol, apart from the expected methacrolein and acetic acid, the formation of *i*-butene, 2-butenes, butadiene as well as maleic anhydride was observed.

4. Discussion

The results of oxidation of linear chain and isomeric C_4 molecules on the $(VO)_2P_2O_7$ catalyst presented in Tables 1–3 demonstrate the polyfunctional nature of the VPO catalysts and their ability to selectively oxidize various functions to maleic anhydride. Formation of products shown in Tables 1–3 is explained on the basis of the structural features of the (1 0 0) plane of $(VO)_2P_2O_7$ and the redox chemistry of V^{IV} and V^{V} species.

4.1. Proposed active surface sites

The proposed models of *n*-butane oxidation on the VPO catalysts are based on the dimers of edge-sharing *trans*-oxovanadium(IV) octahedra present in the bulk (1 0 0) plane of $(VO)_2P_2O_7$ [1–4,26,27]. According to the models of Schiøtt et al. [26] and Agaskar et al. [27], the electrophilic vanadyl(IV) oxygen participates in the initial methylene C–H bond activation in *n*-butane and it is subsequently lost during the proposed [4 + 2] cycloaddition of the butadiene intermediate leading to the formation of 2,5-dihydrofuran. However, the review of the redox chemistry of vanadium in its higher oxidation states [28–32] reveals only a few examples of such processes involving the vanadyl oxygen. Moreover, the generation of highly reactive vanadium(IV) and (V) η^1-peroxo or η^2-superoxo species in the presence of molecular oxygen is well known [33–38] and widely used in both stoichiometric and catalytic oxidations of organic molecules [39–41]. In *n*-butane oxidation on the VPO catalysts the catalytic activity is lost when nitrous oxide, a well-known oxotransfer agent [31] is used instead of molecular oxygen [27]. This suggests that the η^1-peroxo or η^2-superoxo species may be involved in the oxidation. In the case of the *trans*-oxovanadium(IV) dimer site proposed as active, the activation of dioxygen would lead to only single peroxo species. Meanwhile, the kinetic studies of *n*-butane oxidation suggest a different site capable of contemporaneous abstraction of two methylene hydrogen atoms in *n*-butane [1,22]. In fact, the (1 0 0) plane of $(VO)_2P_2O_7$ displays chains of *trans*-oxovanadium(IV) dimers running parallel. The *trans*-oxovanadium(IV) dimers are arranged in such a way that the vanadium(IV) atoms with the vacant apical coordination site are always next to each other in a chain. Given the average O–O bond length in vanadium(V) peroxo complexes of 1.5 Å [34], the distance between the oxygen atoms in adjacent peroxo species in a *trans*-oxovanadium(IV) dimer chain (ca. 3.5 Å [42,43]) would compare favorably with the methylene H–H distance in positions 2 and 3 in the eclipsed conformation of *n*-butane (2.3 Å [44]). This suggests that this dimeric site shown in Fig. 1 may be involved in the C–H cleavage in *n*-butane. The present work attempts to offer new pathways of selective oxidation of *n*-butane and other C_4 molecules to maleic anhydride based on such dimeric peroxo site and V^{IV}–V^{V} redox couple.

4.2. Oxidation of unsaturated hydrocarbons

Unsaturated hydrocarbons were much more reactive than *n*-butane. Both 1- and 2-butene underwent isomerization probably catalyzed by surface HPO_4^{2-} or $H_2P_2O_7^{2-}$ groups [3,21,27] and all three isomeric species, i.e. *cis*-, *trans*-2-butene and 1-butene were observed (Fig. 2). The formation of 1,3-butadiene (**3**) is best accounted for by radical abstraction of two allylic H atoms in 2-butene (**1**) by surface (su)peroxo-oxovanadium(V) species belonging to a distant dimeric site (Fig. 1) followed by intramolecular electron transfer and formation of a stable system of conjugated double bonds. Butadiene could either desorb or undergo the [4 + 2] cycloaddition with the surface oxovanadium(V) oxyradical V^{V}–$O^{\bullet}$ to yield 2,5-dihydrofuran (**4**) and the original reduced V^{IV}

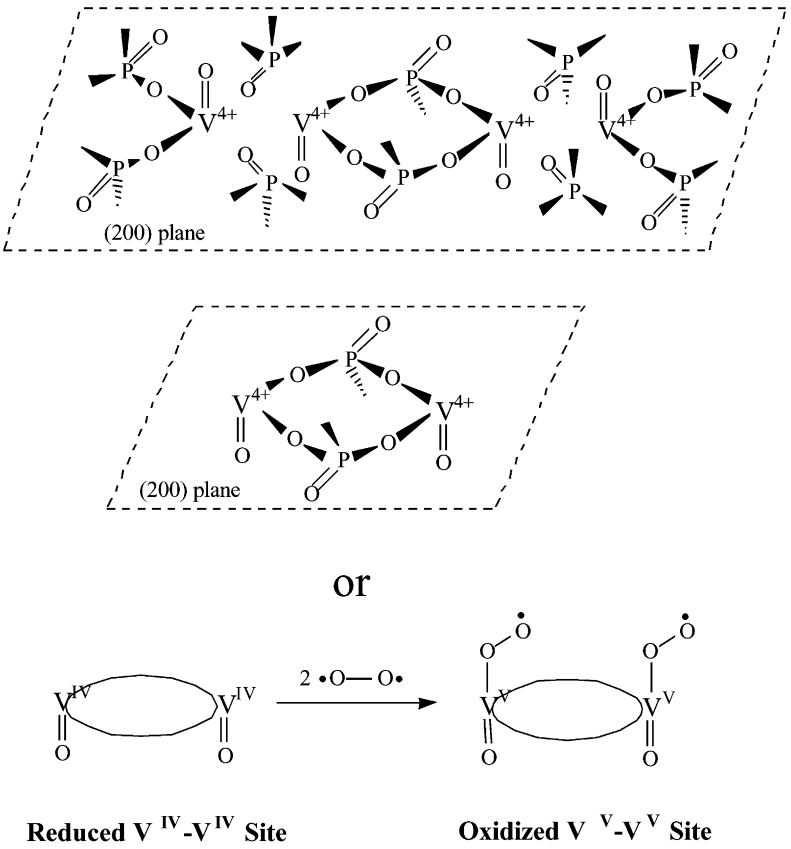

Fig. 1. Proposed *cis*-peroxo-oxovanadium(V) dimeric active site for partial oxidation of hydrocarbons to maleic anhydride over $(VO)_2P_2O_7$ catalyst.

site. The V^{IV} site is then reactivated by dioxygen and maleic anhydride (**5**) is obtained as the result of allylic oxidation in positions 2 and 5 of 2,5-dihydrofuran (Fig. 2).

Another selective path shown in Fig. 2 involves dihydroxylation of the 1,4-alkenyl diradical (**2**) similar to the V_2O_5-catalyzed oxidation of olefins by peroxide [39] or the mechanism proposed by Mimoun et al. for oxidations of aromatics [33]. Such diradical may be stabilized by delocalization of the unpaired electrons through the π-conjugation [45,46]. The unsaturated but-2-ene-1,4-diol (**6**) formed by the abstraction–recombination mechanism [33] then undergoes oxidation by another V^V–$O^•$ site to yield 4-hydroxy-but-2-enal (**7**) and V^{IV}. 4-Hydroxy-but-2-enal similar to other γ-hydroxy-α,β-unsaturated carbonyl compounds can be dehydrated using Lewis or Brönsted acids (e.g. the surface HPO_4^{2-} or $H_2P_2O_7^{2-}$ groups) to form furan (**8**) [47,48], shown in Fig. 2. Furans are well known to undergo cycloaddition with singlet oxygen [49], which is made the basis for the synthesis of 5-hydroxy-2(5*H*)-furanones (**9**) (Fig. 2). The last step involves two consecutive abstractions of hydrogen atom in position 5 and hydroxyl hydrogen by the V^V–$O^•$ species to yield maleic anhydride and V^{IV} site [39–41]. In the case of *i*-butene, no products of skeletal rearrangement were observed, and oxidation of this species gave only the products expected for allylic oxidation and C=C bond scission.

Other partially oxidized species may result from (i) hydration of an olefin followed by oxidation of the alcohol into methylethylketone, and (ii) addition of the peroxo group to the C=C double bonds in a diene and

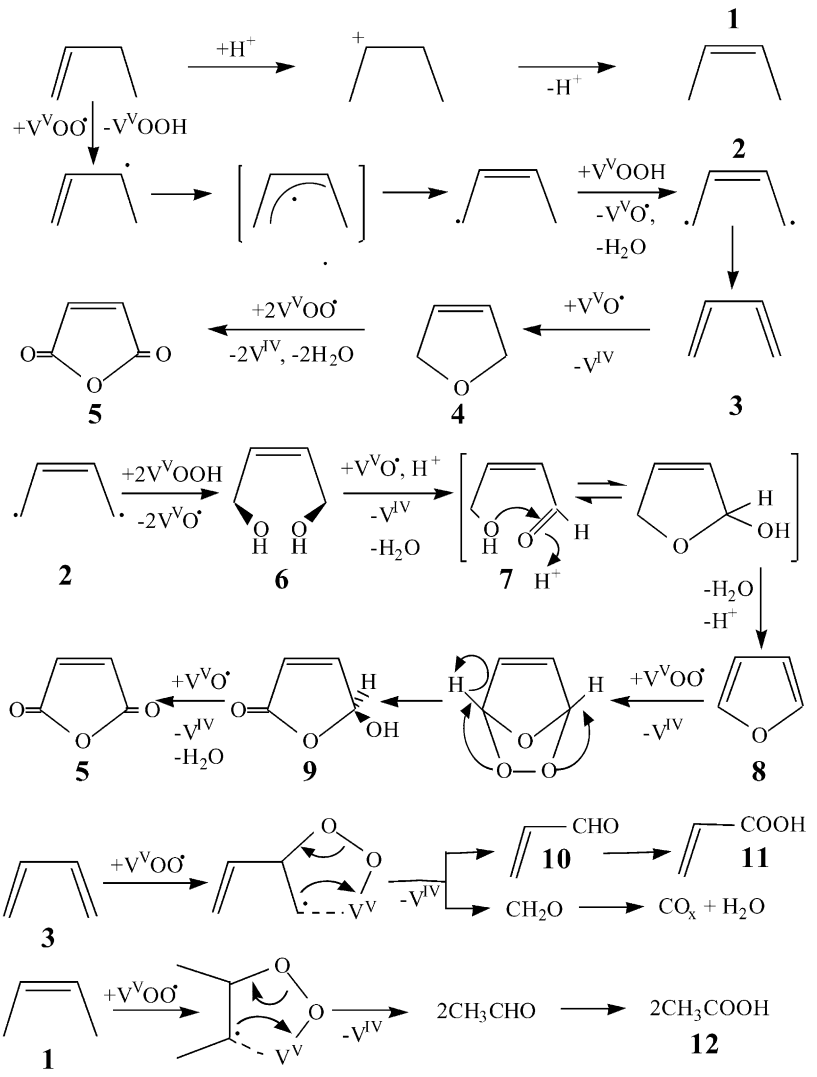

Fig. 2. Proposed oxidation of 1- and 2-butenes over $(VO)_2P_2O_7$ catalyst.

alkene to yield acrylic (**11**) and acetic (**12**) acids, respectively, via decomposition of the peroxymetallocycle (Fig. 2) and further oxidation [39–41].

4.3. Oxidation of five-membered heterocycles

In the case of tetrahydrofuran (**13**), the first step is likely to be H atom abstraction by the peroxo-oxovanadium(V) species in positions 3 and 4 leading to 2,5-dihydrofuran (**4**). Allylic oxidation in positions 2 and 5 of 2,5-dihydrofuran would yield maleic anhydride shown in Fig. 3. This step is likely to occur by the same abstraction–recombination mechanism [33] with the formation of 2,5-diradical, since furan is one of the products of this reaction. In the case of 2,3-dihydrofuran (**14**), the molecule would undergo abstraction of two H atoms in positions 4 and 5 to give furan (**8**), which is then oxidized to MA as shown in more detail in Fig. 2. A competitive allylic oxidation in position 4 and then 5 of 2,3-dihydrofuran would lead to 2,3-dihydrofuran-4,5-dione, a likely precursor to the products of complete oxidation (Fig. 3). This

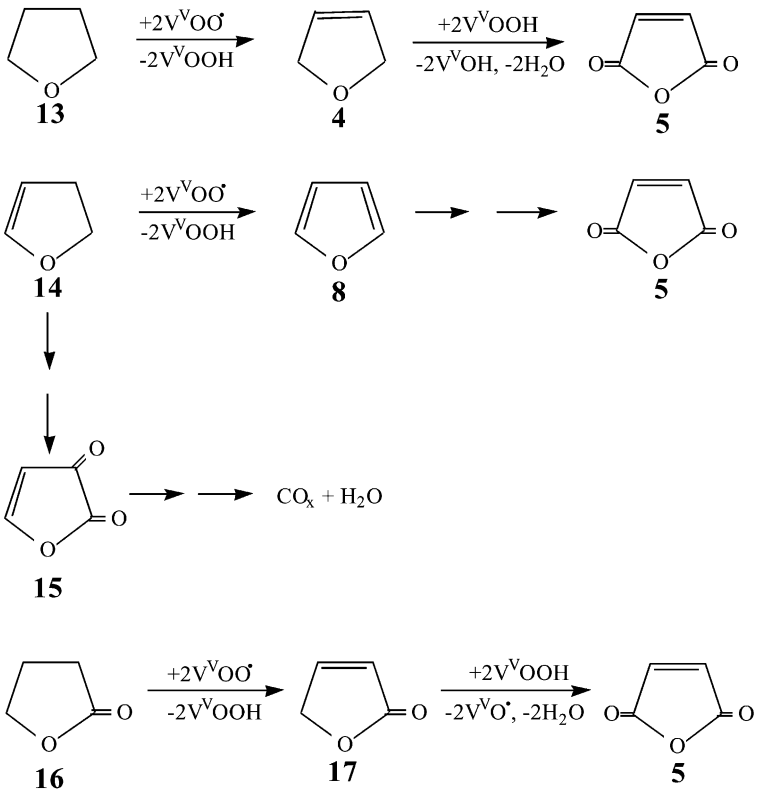

Fig. 3. Proposed oxidation of five-membered heterocycles, tetrahydrofuran, 2,3- and 2,5-dihydrofurans, and γ-butyrolactone over $(VO)_2P_2O_7$ catalyst.

may explain lower selectivity to MA than in the case of 2,5-dihydrofuran. γ-Butyrolactone (**16**) is likely oxidized to MA via 2(5*H*)-furanone (**17**) (Fig. 3).

4.4. Oxidation of alcohols and diols

We have tested the ability of the VPO catalyst to oxidize simple C_4 alcohols to maleic anhydride. The alcohols are first dehydrated to alkenes via formation of carbocations, which is indicated by skeletal rearrangement of the *t*-butyl carbocation in the case of *i*-butanol and formation of linear chain species. The oxidation of the alkenes is then straightforward as shown in Fig. 2.

Oxidation of 1-butanol resulted in the higher yield of maleic anhydride as compared to 2-butanol. This observation may be explained by an access to a "shorter" oxidation path similar to intramolecular cyclization of β- and δ-unbranched primary aliphatic alcohols to 2-alkyl-tetrahydrofurans in nonpolar solvents catalyzed by lead(IV) tetraacetate [39–41,50]. In the case of 1-butanol (**18**) oxidation on the VPO catalysts the 1-butoxy radical (**19**) is generated after the hydroxyl H atom is abstracted by the surface (su)peroxo species (Fig. 4). The intramolecular H atom migration then occurs from the δ-carbon via a quasi-six-membered ring (**20**) [39–41] followed by the H atom loss to the surface peroxide and ring closure to tetrahydrofuran (**13**). Oxidation of tetrahydrofuran to MA proceeds as shown in Fig. 3.

We have observed highly selective oxidation of butanediols, particularly 1,4-diol (Table 3), to maleic anhydride on the VPO catalyst. In the case of 1,4-diol, the yield of MA (ca. 93 mol%) was considerably higher than that of any other C_4 species studied. Several possibilities exist for 1,4-diol cyclization to the five-membered heterocycle (Fig. 5). One the one hand, 1,4-diol (**21**) may be oxidized into γ-butyrolactone (**16**) via 4-hydroxyaldehyde (**22**) and γ-butyrolactol

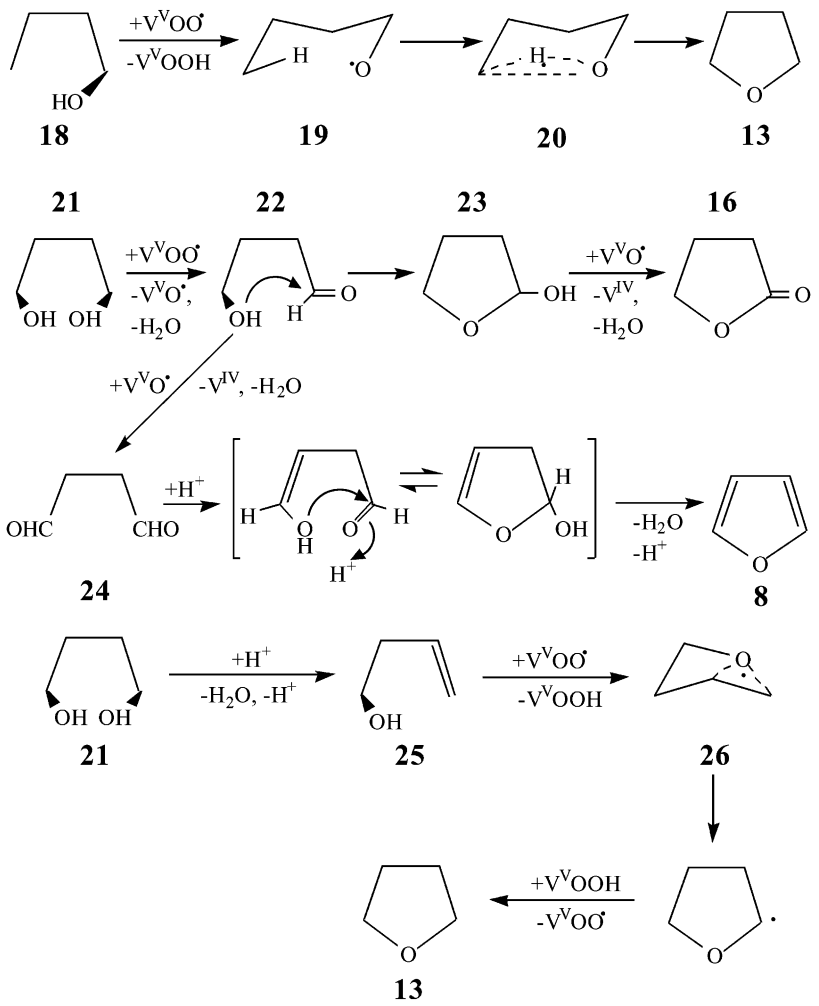

Fig. 4. Proposed oxidation of 1-butanol and 1,4-butanediol over $(VO)_2P_2O_7$ catalyst.

(**23**) [39]. On the other hand, the Paal–Knorr synthesis [51], which involves the cyclizing dehydration of 1,4-dicarbonyl compounds is the most widely used approach to furans. 1,4-Dialdehyde (**24**) formed by oxidation of two hydroxyl groups in 1,4-butanediol provides all of the carbon atoms and the oxygen necessary for the furan nucleus. The process involves addition of the enol oxygen of one carbonyl group to the other carbonyl group, then elimination of water. Finally, a primary Δ^3-alkenol, 3-but-*n*-1-ol (**25**) formed by acid-catalyzed partial dehydration of 1,4-diol, may undergo cyclization to tetrahydrofuran (**13**) by means of intramolecular addition of the oxygen radical to a sterically accessible ethylenic linkage via a π-complex (**26**) [39–41,52] shown in Fig. 5. γ-Butyrolactone, furan and tetrahydrofuran formed in the above reactions are then oxidized to maleic anhydride as shown in Figs. 2 and 3. Dehydration of diols on the VPO catalyst is confirmed by formation of 1,3-butadiene as well as the carbon–carbon bond scission products, ethylene and propylene. Since 1,2- and 1,3-diols cannot undergo cyclization as readily as 1,4-diols [39–41], oxidation of 1,2-butanediol (**27**) and 1,3-butanediol (**28**) to maleic anhydride probably occurs via cyclization of 4-hydroxy-but-2-enal (**7**) to furan (**8**) as shown in Fig. 2. This involves a longer

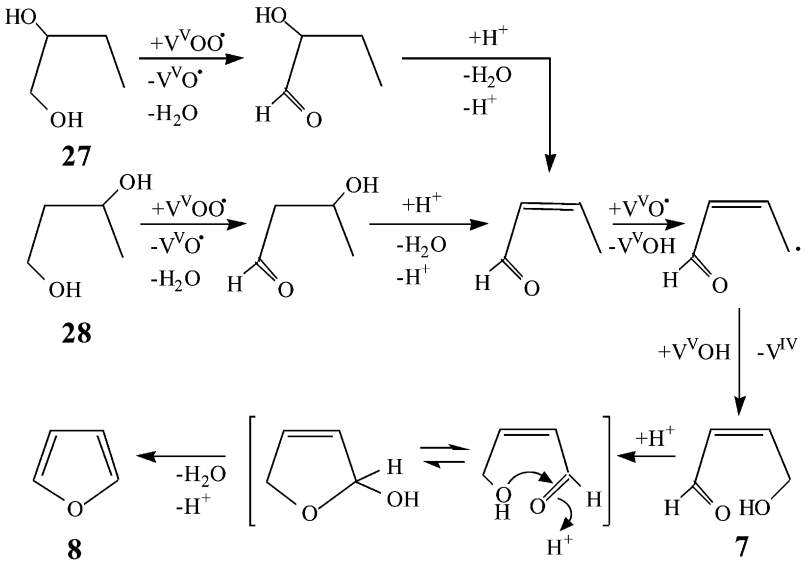

Fig. 5. Proposed oxidation of 1,2- and 1,3-butanediols over $(VO)_2P_2O_7$ catalyst.

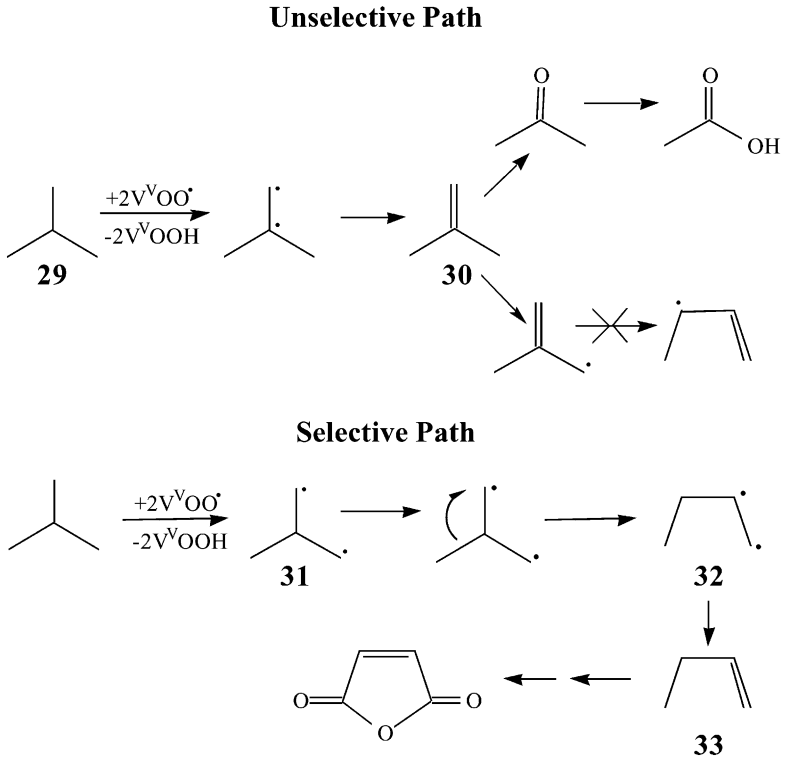

Fig. 6. Proposed oxidation of *i*-butane over $(VO)_2P_2O_7$ catalyst.

reaction pathway and parallel side-reactions (Fig. 5), which may explain lower yield of MA than in the case of 1,4-butanediol.

4.5. Oxidation of i-butane

Oxidation of a branched C_4 alkane, *i*-butane, was carried out to probe the mechanism of the C–H bond activation of alkanes on the VPO catalysts. In the case of *i*-butane (**29**) the surface-bound peroxo radical would show discrimination in activating first the weaker tertiary C–H bond (Fig. 6). The hydroxylation of the *t*-butyl radical would lead to *t*-butanol [33]. Formation of methacrolein and methacrylic acid (Table 1) may be explained by allylic oxidation of *i*-butene obtained by dehydration of *t*-butanol. The formation of MA is most likely accounted for by the skeletal rearrangement of a carbocation or radical intermediate [53]. The *t*-butyl carbocation would be generated in dehydration of *t*-butanol. However, the three methyl groups inductively delocalize the positive charge on the tertiary carbon atom leading to a stable *t*-butyl carbocation. Therefore, we could not account for formation of MA by the rearrangement of *t*-butyl carbocation to linear 2-butyl carbocation. On the other hand, the activation of both the tertiary and the stronger methyl C–H bonds [39–41] in *i*-butane by the surface-bound peroxo radical would lead via a 1,2-diradical to *i*-butene (**30**) and its oxidation products. No products of skeletal rearrangement would be

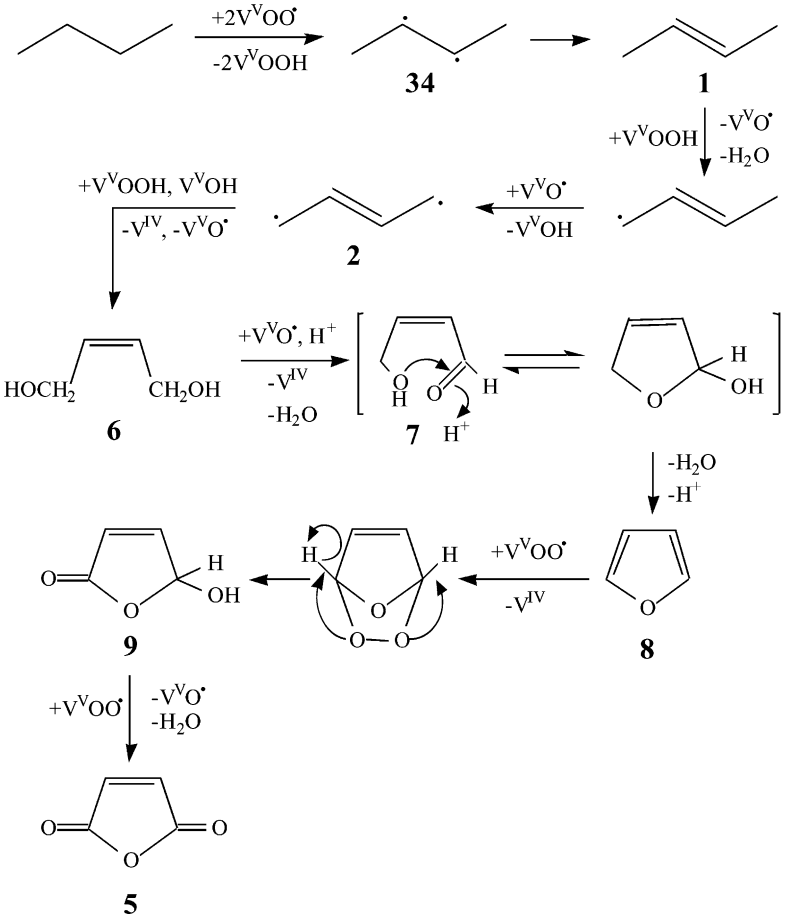

Fig. 7. Proposed oxidation of *n*-butane to maleic anhydride over the *cis*-peroxo-oxovanadium(V) dimer sites present in the (1 0 0) planes of $(VO)_2P_2O_7$.

expected in this case either. The formation of maleic anhydride in the *i*-butane oxidation may be explained by a reaction pathway involving the abstraction of the two hydrogen atoms in positions 1 and 3. Activation of the two methyl C–H bonds would occur to some extent resulting in the formation of a 1,3-diradical (**31**). Simple radicals undergo skeletal rearrangement only when migrating group is aromatic capable of delocalizing an extra electron in the π-system [53]. However, in the case of *t*-butyl 1,3-diradical skeletal rearrangement via methyl group migration and a cyclic intermediate (Fig. 6) is well-documented [45,53] leading to linear 1,2-diradical (**32**) and 1-butene (**33**). Formation of maleic anhydride during *i*-butane oxidation on the VPO catalyst (Table 1) suggests that such skeletal rearrangement does occur. On the other hand, it also indicates that the activation of alkanes on the VPO catalysts may proceed via contemporaneous homolytic C–H bond cleavage and formation of a diradical intermediate.

4.6. Oxidation of n-butane

We propose here a mechanism of *n*-butane oxidation on the VPO catalysts (Fig. 7) based on the formation of the 2,3-diradical (**34**) and further steps of its oxidation to maleic anhydride consistent with the results of oxidation of various C_4 species (Tables 1–3 and Figs. 2–6). 2-Butene undergoes dihydroxylation by abstraction–recombination mechanism via 1,4-alkenyl diradical (**2**) (Figs. 2 and 7). Olefinic and π-allyl intermediates have been previously detected in the in situ IR studies of oxidation of C_4 hydrocarbons, including *n*-butane, over the VPO catalysts [54–56]. The unsaturated but-2-ene-1,4-diol (**6**) thus formed then undergoes oxidation by another V^{V}–$O^{\bullet}$ site to yield 4-hydroxy-but-2-enal (**7**) and V^{IV}. 4-Hydroxy-but-2-enal is dehydrated by the surface HPO_4^{2-} or $H_2P_2O_7^{2-}$ groups to form furan (**8**). Furan undergoes cycloaddition with singlet oxygen to yield 5-hydroxy-2(5*H*)-furanones (**9**) which is oxidized to maleic anhydride by the V^{V}–$O^{\bullet}$ species as shown in Figs. 2 and 7.

5. Conclusions

We have studied partial oxidation of 16 C_4 probe molecules to maleic anhydride over the $(VO)_2P_2O_7$ catalyst. The results reveal that in addition to species that have been previously studied [1–3,21], the butanols and butanediols can also be selectively oxidized into maleic anhydride. This demonstrates the existence of new selective oxidation pathways of organic molecules over the VPO catalysts. The oxidation of 1,4-butanediol is remarkably selective. The observation of unusually high yield of maleic anhydride in this case (93 mol%) may be of interest from a commercial viewpoint, although the reduction of maleic anhydride is currently one of the industrial methods for manufacturing 1,4-butanediol [57].

On the other hand, the oxidation of these probe molecules provided insights into the mechanism of *n*-butane oxidation. We have proposed a mechanism for partial oxidation of *n*-butane to maleic anhydride by the *cis*-(su)peroxo-oxovanadium(V) dimeric site present in the oxidized (1 0 0) surface of $(VO)_2P_2O_7$. The proposed model is consistent with both the redox behavior of vanadium in the oxidation states IV and V and the results of partial oxidation of probe molecules obtained in the present and previous studies.

References

[1] G. Centi, F. Trifirò, J.R. Ebner, V.M. Franchetti, Chem. Rev. 88 (1988) 55.
[2] P. Ruiz, B. Delmon (Eds.), Proceedings of the 1st Symposium on New Developments in Selective Oxidation, Catal. Today 1 (2) (1987) 475.
[3] G. Centi (Ed.), Proceedings of the Vanadyl Pyrophosphate Catalysts, Vol. 16, Elsevier, Amsterdam, 1993, pp. 1–154.
[4] V.V. Guliants, J.B. Benziger, S. Sundaresan, I.E. Wachs, J.-M. Jehng, J.E. Roberts, Catal. Today 28 (1996) 275.
[5] V.V. Guliants, J.B. Benziger, S. Sundaresan, I.E. Wachs, N. Yao, Catal. Lett. 32 (1995) 379.
[6] Z.-Y. Xue, G.L. Schrader, J. Phys. Chem. B 103 (1999) 9459.
[7] E. Bordes, Catal. Today 1 (1987) 499 and references therein.
[8] G. Bergeret, M. David, J.P. Broyer, J.C. Volta, G. Hecquet, Catal. Today 1 (1987) 37 and references therein.
[9] N. Harrouch Batis, H. Batis, A. Ghorbel, J.C. Vedrine, J.C. Volta, J. Catal. 128 (1991) 248.
[10] N. Yamazoe, H. Morishige, J. Tamaki, N. Miura, in: L. Guczi, et al. (Eds.), New Frontiers in Catalysis, Elsevier, Amsterdam, 1993, p. 1979.
[11] M.T. Sananes, A. Tuel, J.C. Volta, J. Catal. 145 (1994) 251.
[12] G. Koyano, T. Okuhara, M. Misono, J. Am. Chem. Soc. 120 (1998) 767.
[13] P.L. Gai, K. Kourtakis, Science 267 (1995) 661.
[14] P.L. Gai, Acta Crystallogr. B 53 (1997) 346.
[15] F. Cavani, F. Trifirò, Chemtech 24 (1994) 18.
[16] J.R. Ebner, M.R. Thompson, Catal. Today 16 (1993) 51.

[17] G.J. Hutchings, C.J. Kiely, M.T. Sananes-Schulz, A. Burrows, J.C. Volta, Catal. Today 40 (1998) 273.
[18] U. Rodemerck, B. Kubias, H.-W. Zanthoff, M. Baerns, Appl. Catal. A. 153 (1997) 203.
[19] U. Rodemerck, B. Kubias, H.-W. Zanthoff, G.-U. Wolf, M. Baerns, Appl. Catal. A. 153 (1997) 217.
[20] D. Wang, H.H. Kung, M. Barteau, Appl. Catal. A 201 (2000) 203.
[21] F. Cavani, F. Trifirò, Catalysis 11 (1994) 246.
[22] M.A. Pepera, J.L. Callahan, M.J. Desmond, E.C. Milberger, P.R. Blum, N.J. Bremer, J. Am. Chem. Soc. 107 (1985) 4883.
[23] V.V. Guliants, Catal. Today 51 (1999) 255.
[24] Y. Schuurman, J.T. Gleaves, Ind. Eng. Chem. Res. 33 (1994) 2935.
[25] H.E. Bergna, US Patent 4,769,477 (1988), to E.I. Du Pont de Nemours and Co., Wilmington, DE.
[26] B. Schiøtt, K.A. Jørgensen, R. Hoffmann, J. Phys. Chem. 95 (1991) 2297.
[27] P.A. Agaskar, L. DeCaul, R.K. Grasselli, Catal. Lett. 23 (1994) 339.
[28] A. Butler, C.J. Carrano, Coord. Chem. Rev. 109 (1991) 61 and references therein.
[29] D. Rehder, in: H. Sigel, A. Sigel (Eds.), Metal Ions in Biological Systems: Vanadium and its Role in Life, Vol. 31, Marcel Dekker, New York, 1995, p. 249.
[30] D. Rehder, Angew. Chem. Int. Ed. 30 (1991) 148.
[31] R.H. Holm, Chem. Rev. 87 (1987) 1401 and references therein.
[32] A. Butler, in: N.D. Chasteen (Ed.), Vanadium in Biological Systems, Kluwer, Dordrecht, The Netherlands, 1990, p. 25.
[33] H. Mimoun, L. Saussine, E. Daire, M. Postel, J. Fischer, R. Weiss, J. Am. Chem. Soc. 105 (1983) 3101.
[34] A. Butler, M.J. Clague, G.E. Meister, Chem. Rev. 94 (1994) 625 and references therein.
[35] H. Mimoun, M. Mignard, P. Brechot, L. Saussine, J. Am. Chem. Soc. 108 (1986) 3711.
[36] K.B. Sharpless, T.R. Verhoeven, Aldrichim. Acta 12 (1979) 63.
[37] G.B. Shul'pin, D. Attanasio, L. Suber, J. Catal. 142 (1993) 147.
[38] M. Bonchio, V. Conte, F. Di Furia, G. Modena, J. Org. Chem. 54 (1989) 4368.
[39] W.J. Mijs, C.R.H.I. de Jonge (Eds.), Organic Synthesis by Oxidation with Metal Compounds, Plenum Press, New York, 1986.
[40] R.A. Sheldon, J.K. Kochi, Metal Catalyzed Oxidations of Organic Compounds, Academic Press, New York, 1981.
[41] W.A. Waters, J.S. Littler, in: K.B. Wiberg (Ed.), Oxidation in Organic Chemistry, Part A, Academic Press, New York, 1965, p. 185.
[42] S. Linde, L. Gorbunova, Dokl. Akad. Nauk SSSR 245 (1979) 584.
[43] P.T. Nguyen, R.D. Hoffman, A.W. Sleight, Mater. Res. Bull. 30 (1995) 1055.
[44] R.C. Weast, M.J. Astle, W.H. Beyer (Eds.), CRC Handbook of Chemistry and Physics: a Ready-Reference Book of Chemical and Physical Data, 67th Edition, CRC Press, Boca Raton, FL, 1986.
[45] W.T. Borden (Ed.), Diradicals, Wiley/Interscience, New York, 1982.
[46] A. Rajca, Chem. Rev. 94 (1994) 871.
[47] J.A. Joule, K. Mills, G.F. Smith, Heterocyclic Chemistry, 3rd Edition, Chapman & Hall, London, 1995.
[48] N. Clauson-Kaas, Acta Chem. Scand. 15 (1961) 1177.
[49] A.A. Gorman, G. Lovering, M.A.J. Rodgers, J. Am. Chem. Soc. 101 (1979) 3050.
[50] R.E.J. Partch, Org. Chem. 30 (1965) 2498.
[51] L.T. Scott, J.O. Naples, Synthesis (1973) 209.
[52] S. Konstantinovic, Z. Bugarcic, S. Milosavljevic, G. Schroth, M. Mihailovic, Liebigs Ann. Chem. (1992) 261.
[53] J. March, Advanced Organic Chemistry, 4th Edition, Wiley, New York, 1992.
[54] R.W. Wenig, G.L. Schrader, J. Phys. Chem. 90 (1986) 6480.
[55] S.J. Puttock, C.H. Rochester, J. Chem. Soc., Faraday Trans. I 82 (1986) 3033.
[56] R.W. Wenig, G.L. Schrader, J. Phys. Chem. 91 (1987) 1911.
[57] J.I. Kroschwitz, M. Howe-Grant (Eds.), Encyclopedia of Chemical Technology, Wiley, New York, 1991.